J Biomol NMR (2010) 47:289–295
DOI 10.1007/s10858-010-9428-6

NMR STRUCTURE NOTE

NMR structure note: oxidized microsomal human cytochrome b5

Marcela Nunez · Eric Guittet · Denis Pompon · Carine van Heijenoort · Gilles Truan

Received: 7 May 2010 / Accepted: 11 May 2010 / Published online: 8 June 2010

Keywords NMR structure · Cytochrome b5 · Electron transport protein

Abbreviations

CSI	Chemical shift index
cytb5	Cytochrome b_5
Mc	Microsomal
OM	Outer membrane mitochondrial
Hb5s	Soluble part of human cytochrome b_5
HBP	Heme binding pocket
nOe	Nuclear Overhauser effect
ppm	Part per million
RMSD	Root mean square deviation

Biological context

Cytochrome b_5 (cytb5) is a small membrane-bound hemoprotein present in all eukaryotic organisms. In most eukaryotic cells, cytb5 is attached to the cytosolic face of the endoplasmic reticulum and is described as the microsomal form (Mc). In vertebrates, two supplementary cytb5 can be found: soluble in the erythrocytes and membrane-bound attached to the internal face of the outer membrane in the mitochondria (OM) (Wang et al. 2007). Cytb5 can be divided into three domains: an N-terminal hydrosoluble globular domain that contains approximately 90 residues, a C-terminal hydrophobic domain about 25 residues long and a linker between the two above-mentioned domains. The hydrophilic domain contains the redox center, an iron protoporphyrin IX, ligated to the apoprotein by two histidyl residues.

Mc cytb5 transfers electrons to various acceptors and is consequently involved in many different metabolic pathways. In the mixed function oxidase system, Mc cytb5 is a facultative electron donor to cytochromes P450 (Vergeres and Waskell 1995). Several mechanisms for the recognition between cytb5 and its physiological or artificial acceptors have been hypothesized. The implication of electrostatic interactions has been mostly studied with the cytochromes P450 as acceptors and is now widely accepted as a dominant factor (Schenkman et al. 1994). Nonetheless, several other factors may contribute positively to the recognition mechanism. First, the soluble domain of cytb5 lacking its C-terminal membrane domain cannot transfer electrons to membrane electron acceptors like cytochrome P450 (Dailey and Strittmatter 1978) while the full-length cytb5 can transfer electrons to both soluble and membrane-bound electron acceptor proteins (Vergeres and Waskell 1995). The linker is also recognized as an important factor controlling cytb5 to P450 interactions (Clarke et al. 2004).

The three dimensional structures of the oxidized or reduced soluble domain of wild-type and mutant cytb5 from different species have been determined, either by X-ray or NMR. So far, no three dimensional structure of the full length protein has been reported, although some solid-state NMR data of the full-length rabbit cytb5 inserted in bicelles was

Electronic supplementary material The online version of this article (doi:10.1007/s10858-010-9428-6) contains supplementary material, which is available to authorized users.

M. Nunez · D. Pompon · G. Truan (✉)
Centre de Génétique Moléculaire, CNRS, Av. de la Terrasse, Gif-sur-Yvette 91198, France
e-mail: gilles.truan@cgm.cnrs-gif.fr

E. Guittet · C. van Heijenoort (✉)
Institut de Chimie de Substances Naturelles, CNRS, av. de la Terrasse, Gif-sur-Yvette 91198, France
e-mail: carine@icsn.cnrs-gif.fr

recently described (Xu et al. 2008). All the reported tertiary structures show a conserved fold featuring six alpha helices and one beta-sheet. The heme-binding pocket (HBP) is composed of the beta-sheet and a four-helix bundle delimitating a crevice. Two loops connecting the helices of the bundle contain the two strictly conserved histidyl residues that are the axial ligands of the heme iron. The iron protoporphyrin IX being an asymmetric molecule, its insertion in cytb5 can be found in two distinct orientations noted A and B form. Several groups have reported that the side-chain nature and positioning of the residues in the HBP influence the relative A to B ratios (Altuve et al. 2001; Banci et al. 2000; Cowley et al. 2002; Sun et al. 2005). Despite these differences, the tertiary structure of the globular domain of cytb5 is highly conserved throughout the different species. The linker part of cytb5 is not present in the majority of determined tertiary structures except for the 1HKO (Muskett et al. 1996). The main feature of this linker segment is a total absence of secondary structure even when present in its complete form (up to the membrane segment). A careful examination of the cytb5 alignment shows that the linker segment is clearly the less conserved part of the cytb5 sequence, contrarily to the hydrosoluble domain in the different cytb5 from different origins. We report here the structural analysis of the soluble part of human cytb5 (Hb5 s) comprising the heme domain and the full-length linker.

Methods and results

Protein expression and purification

The gene coding for the hydrophilic domain and linker segment (108 residues) of Hb5 s was cloned into the vector pET-15b (Novagen). Uniformly ^{15}N and $^{15}N/^{13}C$ labeled protein were expressed in *E. coli* BL21 (DE3) using M9 minimal media containing $^{15}NH_4Cl$ and ^{13}C-glucose. Protein was purified using a nickel-column (Hi-Trap, GE HealthCare) followed by an ion exchange column (DEAE-Sepharose Fast Flow, GE HealthCare) and finally a gel filtration column (Sephacryl S-200, GE HealthCare). Hb5 s purity was checked by UV Visible spectroscopy (ratio of the absorbance at 412 nm versus 280 nm above 4.0). Purity was also checked on SDS PAGE. Samples were concentrated using an Amicon Concentrator (Millipore) to a final concentration of $\sim$1 mM. Samples used for NMR spectroscopy contained 10 mM sodium/potassium phosphate buffer pH 6.5 in either 10% D_2O/90% H_2O or in 100% D_2O.

NMR spectroscopy

NMR spectra were acquired at 308 K on NMR Bruker Avance 600, 700 or 800 spectrometers. Backbone resonance assignment was obtained from the analysis of ^{15}N-HSQC, ^{13}C-HSQC, HNCO, HNCA, HN(CO)CA, CBCANH, CBCA(CO)NH COCAHA, 3D ^{1}H-^{15}N NO ESY-HSQC and 3D ^{1}H-^{15}N HOHAHA-HSQC. For side-chain assignment, HCCH-COSY and HCCH-TOCSY spectra for aliphatics and aromatics resonances were acquired. Spectra were processed by the Bruker software Xwin-NMR or NMRPipe and analyzed using Sparky (Goddard and Kneller). nOe distance restraints were obtained from 3D-[^{1}H,^{15}N]-NOESY-HSQC (mixing time 150 ms), 3D-[^{1}H-^{13}C]-NOESY-HSQC for aromatic and aliphatic resonances (mixing time 80 ms) and 2D-^{1}H NOESY in D_2O (mixing time 150 ms). nOe distance restraints between the heme and the protein protons were obtained using a 2D-^{1}H NOESY in D_2O.

The backbone dynamic of the protein was monitored by ^{15}N relaxation using classical pulse sequences. 18 experiments with 16 relaxation delays were acquired for $R_1(^{15}N_z)$ determination (20($\times$2), 40($\times$2), 60, 80, 100, 120, 150, 200, 250, 300, 400, 500, 800, 1000, 1500 and 2000 ms). The $R_1(^{15}N_{x,y})$ values were determined from 16 experiments with 13 relaxation delays (16, 32 ($\times$4), 48, 64, 80, 96, 112, 144, 160, 208, 256, 320, 428 ms). Cross-peak integration was performed using NMR View. Relaxation rates were evaluated using classical fitting procedures written in Matlab. For $^{1}H- > {}^{15}N$ heteronuclear nOes, the relaxation delay was set to 5 s and proton saturation was achieved with a GARP sequence during 4 s.

Backbone torsion angles ϕ and ψ were predicted by TALOS (Cornilescu et al. 1999) from $^{1}H^{N}$, ^{15}N, $^{1}H_{\alpha}$, ^{13}CO, $^{13}C_{\alpha}$ and $^{13}C_{\beta}$ chemical shifts. Backbone hydrogen bond restraints were incorporated in the structure calculation only if they were predicted by CSI and if the corresponding amide protons were in slow exchange with solvent (i.e. still present in the first HSQC recorded after protein lyophilization and dissolving in 100% D_2O) or if β-strand or α-helix characteristic nOe cross-peaks were observed. Each hydrogen bond in β-strand was enforced by two distances restraints of 1.2–3.7 Å between the amide nitrogen and the carboxyl oxygen and of 1.2–2.7 Å between the amide proton and the carboxyl oxygen.

Resonances assignment

Protein NMR resonances assignment was achieved for 97% of the backbone and side-chains atoms using Sparky software (Goddard and Kneller). It was deposited in the BMRB (deposit number 6921). Heme protons assignment was obtained from comparison between the previously reported chemical shift in cytb5 (Lee et al. 1990) and from the analysis of a 2D-NOESY ^{12}C filtered spectra recorded in 100% D_2O. Chemical shifts of the globular domain are in

good agreement with those previously published (BMRB entry 5745, 4130, 4602 and 294 respectively for bovine, rat, rabbit and calf). Some discrepancies can however be noted for conserved residues in four specific regions: Y55-T58, E63-G67, V86-H88 and L71-R72. The TALOS program predicted 47 ϕ and ψ backbone torsion angle restraints and identified the secondary structure elements based on the chemical shifts obtained. These restraints were confirmed by the nOe patterns.

Tertiary structure calculation

The tertiary structure calculation was carried out using Aria 1.2 (Linge et al. 2001, 2003). Heme was bound to the protein through one covalent bond between the Nε2 of His 64 and the heme iron atom, thus defining a new residue, HIX, which comprises H64 and the heme. The geometrical parameters for this residue were imposed according to the values in the NMR structure of the soluble bovine cytb5 (bond length of 2.2 Å for the pseudo-bond between histidine Nε2 and heme–iron, and definition of eight angles between Nε2 and Fe atoms). All force constants and molecular parameters were set to their default values except for the HIX residue constants whose values were obtained from Xplor2D (Kleywegt and Jones 1998).

Simulated annealing was performed with 10,000 steps at 2000 K followed by 1000 cooling steps down to 1000 K and 4000 steps down to a final temperature of 50 K. Finally, these structures were energy minimized using 4000 steps of Powell energy minimization. A total of 540 structures were calculated in 8 iterations. The 20 lowest energy structures were subjected to a final minimization in water. The quality of the final structures was evaluated using PROCHECK_NMR (v.3.5.4) (Laskowski et al. 1996).

Hb5s three-dimensional structure was calculated using 1726 nOes-derived distances constraints, 49 hydrogen bonds and 94 dihedrals angles estimated by the TALOS software. The energetic and structural statistics are listed in Table 1. In the calculation, no nOe constraints > 0.5 Å were violated. The RMSD values with respect to the mean structure for residues implied in secondary structures are equal to 0.58 and 1.08 Å for backbone and all heavy atoms, respectively. Globally, 66.7% of the residues in the well-defined region of the protein are in the most favored region of the Ramachandran diagram, whereas 24.8% belong to an allowed region, 4.3% in a generously allowed region and 4.3% in a disallowed region.

Hb5s tertiary structure has been deposited in the Protein Data Bank under the accession number 2I96 and is composed of the 20 best (lowest energy) calculated structures (Fig. 1). The numbering of Hb5s structure starts at the residue 21 because of the N-terminus histidine tag (this numbering will be used throughout the entire paper). Hb5s structure contains 4 α-helices: α_1 33-38, α_3 68-73, α_4 80-86, α_5 89-96 and 5 β-strands: β_1 31–32, β_2 41–42, β_3 45–49, β_4 53–56 and β_5 100–104. The β-strands exhibit low RMSD values (<0.5 Å). The lowest value is obtained for β_3 which is in the middle of the protein tertiary structure and this in agreement with the observed slow deuterium-exchange rate constants. The fifth helix present in previously published cytb5 structures was not detected by the PROCHECK software during deposition in the RCSB data bank. However, nOe connectivities, CSI and TALOS (Fig. 2A) indicate the presence of a helix (α_2) from residue 58 to residue 63. This ensemble of secondary structures (α_2–α_5 and the β-sheet) forms the heme binding-pocket (HBP). The RMSD value for the helices (1 to 5) is 0.93 Å.

Table 1 Structural statistics

Experimental restraints	
Total nOes	1726
Intra-residue	802
Sequential	279
Medium	197
Long range	447
Restraints statistics	
RMSD from standard geometry	
Bond (Å)	0.0045 ± 0.0003
Angle (°)	1.52 ± 0.001
Dihedral (°)	43.98 ± 0.30
Improper (°)	2.92 ± 0.11
Energies of final structures (kcal mol^{-1})	
E_{BOND}	44.62 ± 6.51
F_{ANGLE}	1375.1 ± 18.7
F_{VDW}	−1034.3 ± 19.6
F_{IMP}	1747.4 ± 107.3
F_{nOe}	50.43 ± 52.53
F_{TOT}	−1534.5 ± 105.9
Ramachandran plot (2I96/1AW3/1DO9/1HKO*)	
Most favored	66.7/69.9/67.7/70.8
Allowed	24.8/22.9/26/23.2
Generously	4.3/1.2/5.5/2.5
Disallowed	4.3/6.0/0.8/3.4
RMSD backbone, 2nd structure (Å)	0.58 ± 0.09
RMSD heavy atoms, 2nd structure (Å)	1.08 ± 0.09
nOe violations > 0.5 Å	0
nOe violations > 0.3 Å	1

The respective energy term (F_{BOND}, F_{ANGLE}, F_{VDW}, F_{IMP}, F_{nOe}, F_{CDIH}, F_{TOT}) are expressed in kcal mol^{-1}. F_{TOT} is the potential energy; F_{BOND}, F_{ANGLE}, and F_{IMP} are the potential energy related to covalent geometry and interaction; F_{VDW} is the energy due to the Van der Waals interactions and F_{nOe}, the energy due to the distance restraint violations. 2I96, 1AW3, 1DO9 and 1HKO are the pdb ID of oxidized human, rat, rabbit and bovine cytochrome b5

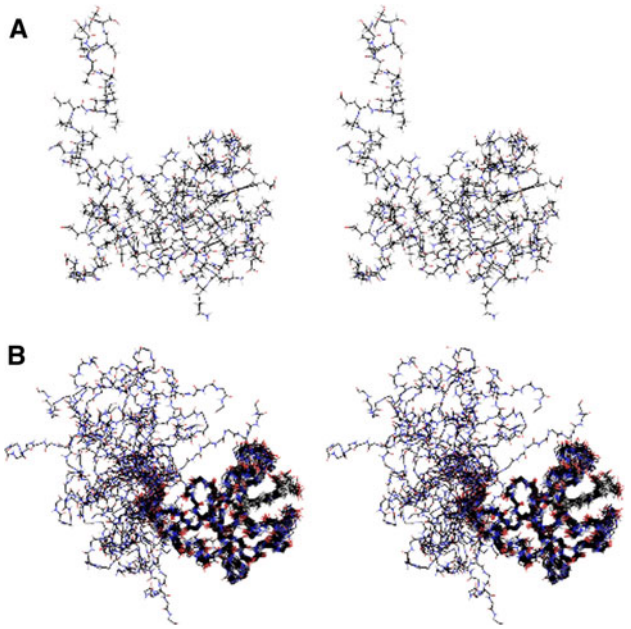

Fig. 1 Representation of Hb5s structure. **a** Stereo trace of the model 1 of Hb5s structure. **b** Stereo trace of the backbones of the 20 models of Hb5s structure. The figure was realized with Pymol (http://www.pymol.org)

Discussion and conclusions

Dynamic analysis of the hydrophilic domain of Hb5s

Heteronuclear nOe, $R_1(^{15}N_z)$ and $R_2(^{15}N_{x,y})$ values are presented in Fig. 2B. The analysis of the heteronuclear nOe values show that residues at the C-terminal fragment corresponding to the linker (residues 105-128) are highly flexible. Otherwise, the core of the protein (residues 30-104) appears quite rigid with heteronuclear nOe values around 0.8, except for L57 and H88. The mean relaxation rates values of $R_1(^{15}N_z)$, $R_2(^{15}N_{x,y})$ and nOes($^1H^N- > ^{15}N$) are $1.84 \pm 0.25\ s^{-1}$, $7.4 \pm 1.7\ s^{-1}$ and 0.65 ± 0.40, respectively, along the whole protein and $1.87 \pm 0.24\ s^{-1}$, $7.7 \pm 1.5\ s^{-1}$ and 0.75 ± 0.05, respectively, in the structured region (32–108). H88 flexibility revealed in heteronuclear nOe is confirmed by its $R_2(^{15}N_{x,y})$ value. The higher than the mean $R_1(^{15}N_z)$ and $R_2(^{15}N_{x,y})$ values of T90 can be explained by its proximity with the paramagnetic center. As a conclusion, the hydrophilic domain of human Mc cytb5 is quite rigid except for some punctual residues which present movements in the hundreds of picoseconds time scale, like H88 and L57, or in the μs-ms rate scale, like H52. The two axial ligands of the heme, H88 and H64 undergo different internal dynamics, H88 being more flexible than H64. It has been suggested previously that the heme release from cytb5 occurs primarily at the histidine residue closer to the C-terminal end (Ihara et al. 2000). The dynamic of H88 could then be related to the better potentiality of the heme release from this histidine compared to the other. The flexibility of L57 might be related to its hinge location between strand β_3 and helix α_2 and this position could act as a bridgehead allowing the support of the β-sheet stability in front of α_2 rearrangements.

Comparison of Hb5s secondary structure elements with other isoforms

Figure 3a shows the secondary structure elements positioned over an alignment of four mammal's cytb5 sequences derived from the PDB (rat, bovine, rabbit and human). The hydrophilic domain of cytb5 is characterized by short (5–10 residues) secondary structure elements. The RMSD for the backbone atoms of the hydrophilic domain between the average Hb5s structure (residues 30–104) and the other average solution structure is small: 1.15 Å for Mc bovine cytb5 (1HKO), 1.02 Å for Mc rabbit cytb5 (1DO9) and 1.15 Å for Mc rat cytb5 (1AW3). Thus, the tertiary structure of the central part of the hydrophilic domain of Hb5s is highly similar to the other mammalian Mc cytb5 tertiary structures. A comparison of RMSD between the various secondary structure elements is presented in the Table 1 of the Supplementary Material.

On the contrary, RMSD values for α-helices are >0.4 Å and their lengths vary between the different isoforms (Fig. 3b). Helix α_2 may adopt different positions and orientations compared to other cytb5. Hb5 s has a methionine at position 70 instead of a leucine in other mammals (Fig. 3a). This residue may disrupt the hydrophobic network formed between helices α_5 and α_2, leading to a decrease in the steric interaction between heme substituents and residues side-chains. The modification of the hydrophobic interactions between these two helices could also be at the origin of the partial α_2 misfolding. This supposition is in agreement with the relaxation data of L57 (Fig. 2A). This type of dynamics was already described in the rat cytb5 (Dangi et al. 1998), although the α_2 helix is well conformed in the rat cytb5 compared to the human form. Finally, α_4 and α_5 are the most conserved helices (RMSD < 1 Å).

Heme binding and orientation

Heme in cytb5 can be inserted in two opposite orientations that differ by a 180° rotation about the α- and γ-meso heme axis leading to two orientation named A and B. The signal intensity of the ^1H-^{15}N cross peak of residues sensitive to the heme orientation is related to the isomer ratio. In spite of the high identity between hydrophilic domains of the different cytb5, this isomer ratio varies among species: 1.5:1, 5:1 and 9:1 for rat, rabbit and bovine cytb5, respectively. It was proposed that this ratio is modulated by hydrophobic and steric interactions between the heme vinyl

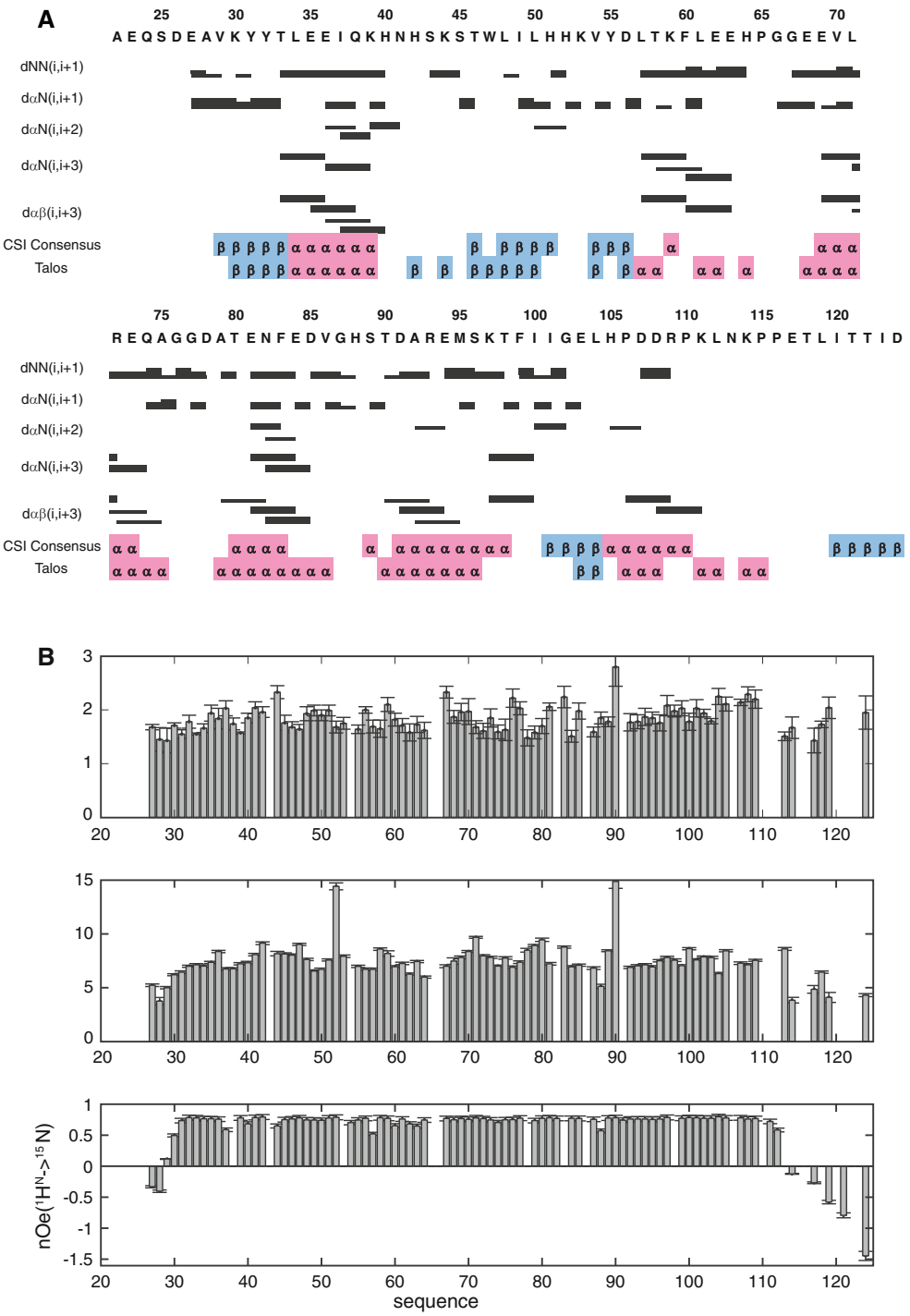

Fig. 2 Secondary structure elements and internal dynamics of Hb5s. **a** Local nOe connectivities, CSI and Talos versus amino acid sequence of Hb5s. **b** (*a*) $R_2(^{15}N_{x,y})$ values, (*b*) $R_1(^{15}N_z)$ values and (*c*) heteronuclear (^1H- > ^{15}N) nOe rates plotted against residue number. Spectra were acquired at 308 K and 700 MHz. Residues discussed in the text are also indicated

and residues L23 and F74 (L48 and F99 in Hb5s) in the rabbit cytb5 structure (Banci et al. 2000). The A/B isomer ratio in Hb5s is 4:1. Residue L48 is identical in all mammals cytb5 and F99 is conserved except for the rat cytb5 where it is replaced by a tyrosine residue. Despite this conservation, the isomer ratio is clearly different between all isoforms. Human cytb5 is different from other mammals cytb5 in the HBP at position 95 (M95 in human vs. leucine in all other species). However, owing to the fact that there is no evident correlation between the nature of these abovementioned residues in the HBP and the relative ratio of A to B forms, it is unclear if M95 influences or not the orientation of the heme in human cytb5.

Linker structure

We report here the second soluble structure of a Mc cytb5 containing the entire linker segment. Cytb5 is attached to

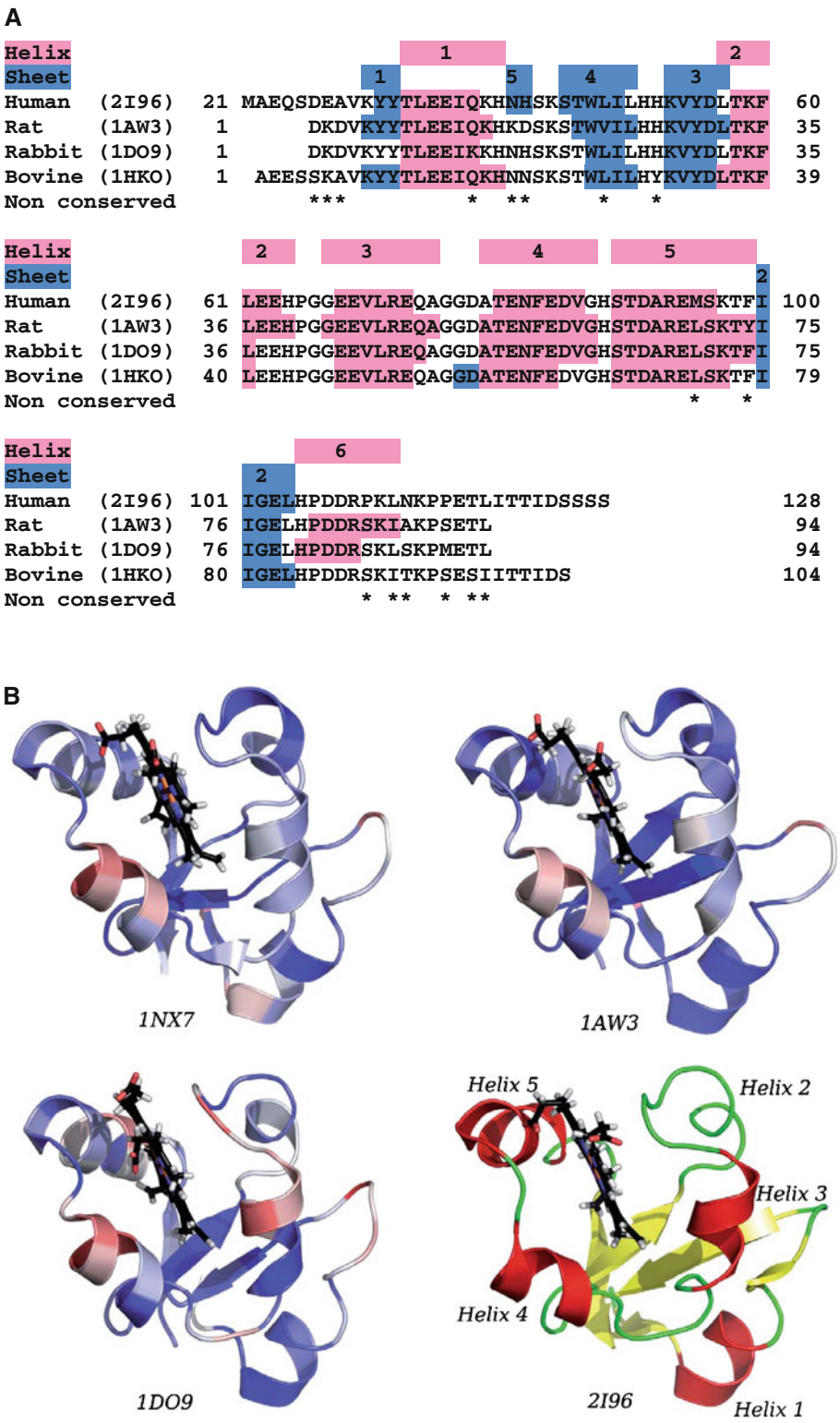

Fig. 3 Summary and variations of secondary structure elements in multiple cytb5. **a** Alignment of primary structures of human, rat, rabbit and bovine cytb5 (sequence derived from the pdb files indicated in *parenthesis*). Secondary structures are indicated by colored boxes (*blue* for strands and pink for helices). The rows Helix and Sheet present the boundaries of secondary structures and their numbering throughout the text. The non conserved positions between the four species are indicated in a separate lane. **b** Ribbon representation of four mammal's cytb5 tertiary structure (1NX7, bovine; 1AW3, rat; 1DO9, rabbit; 2I96, human). Average tertiary structures were aligned, their RMSD at the Cα positions computed and displayed as a color variation from blue (RMSD = 0 Å) to red (RMSD = 3 Å) onto the structure. Hb5s is colored by its secondary structure and the helices are labeled. The figure was realized with Pymol (http://www.pymol.org)

the membrane by a C-terminal anchor. A small connecting peptide (linker) is present between the heme containing domain and the membrane spanning domain. The first report of a cytb5 structure with an entire linker was determined by NMR (Muskett et al. 1996). This structure (1HKO) shows the linker in an extended unfolded conformation. As the identity of the linker protein sequence between mammals Mc cytb5 is of 68%, we decided to verify if this segment could potentially adopt a specific structure in Hb5s. Our data shows an absence of any

secondary structure for the linker, similarly to the reported bovine one, and the dynamics data also confirm this finding (Fig. 1b). The lack of any long distance information for the residues present in the linker can evidently be explained by its flexibility. This of course does not rule out that a defined secondary structure of the linker could be present in the full-length cytb5. The recent advance obtained with solid-state NMR will hopefully be able to address this crucial question (Xu et al. 2008).

References

Altuve A, Silchenko S, Lee KH, Kuczera K et al (2001) Probing the differences between rat liver outer mitochondrial membrane cytochrome b5 and microsomal cytochromes b5. Biochemistry 40:9469–9483

Banci L, Bertini I, Rosato A, Scacchieri S (2000) Solution structure of oxidized microsomal rabbit cytochrome b5. Factors determining the heterogeneous binding of the heme. Eur J Biochem 267: 755–766

Clarke TA, Im SC, Bidwai A, Waskell L (2004) The role of the length and sequence of the linker domain of cytochrome b5 in stimulating cytochrome P450 2B4 catalysis. J Biol Chem 279:36809–36818

Cornilescu G, Delaglio F, Bax A (1999) Protein backbone angle restraints from searching a database for chemical shift and sequence homology. J Biomol NMR 13:289–302

Cowley AB, Altuve A, Kuchment O, Terzyan S et al (2002) Toward engineering the stability and hemin-binding properties of microsomal cytochromes b5 into rat outer mitochondrial membrane cytochrome b5: examining the influence of residues 25 and 71. Biochemistry 41:11566–11581

Dailey HA, Strittmatter P (1978) Structural and functional properties of the membrane binding segment of cytochrome b5. J Biol Chem 253:8203–8209

Dangi B, Sarma S, Yan C, Banville DL et al (1998) The origin of differences in the physical properties of the equilibrium forms of cytochrome b5 revealed through high-resolution NMR structures and backbone dynamic analyses. Biochemistry 37:8289–8302

Ihara M, Takahashi S, Ishimori K, Morishima I (2000) Functions of fluctuation in the heme-binding loops of cytochrome b5 revealed in the process of heme incorporation. Biochemistry 39:5961–5970

Kleywegt GJ, Jones TA (1998) Databases in protein crystallography. Acta Crystallogr D Biol Crystallogr 54:1119–1131

Laskowski RA, Rullmannn JA, MacArthur MW, Kaptein R et al (1996) AQUA and PROCHECK-NMR: programs for checking the quality of protein structures solved by NMR. J Biomol NMR 8:477–486

Lee KB, La Mar GN, Kehres LA, Fujinari EM et al (1990) 1H NMR study of the influence of hydrophobic contacts on protein-prosthetic group recognition in bovine and rat ferricytochrome b5. Biochemistry 29:9623–9631

Linge JP, O'Donoghue SI, Nilges M (2001) Automated assignment of ambiguous nuclear overhauser effects with ARIA. Methods Enzymol 339:71–90

Linge JP, Habeck M, Rieping W, Nilges M (2003) ARIA: automated NOE assignment and NMR structure calculation. Bioinformatics 19:315–316

Muskett FW, Kelly GP, Whitford D (1996) The solution structure of bovine ferricytochrome b5 determined using heteronuclear NMR methods. J Mol Biol 258:172–189

Schenkman JB, Voznesensky AI, Jansson I (1994) Influence of ionic strength on the P450 monooxygenase reaction and role of cytochrome b5 in the process. Arch Biochem Biophys 314: 234–241

Sun N, Wang A, Cowley AB, Altuve A et al (2005) Enhancing the stability of microsomal cytochrome b5: a rational approach informed by comparative studies with the outer mitochondrial membrane isoform. Protein Eng Des Sel 18:571–579

Vergeres G, Waskell L (1995) Cytochrome b5, its functions, structure and membrane topology. Biochimie 77:604–620

Wang L, Cowley AB, Terzyan S, Zhang X et al (2007) Comparison of cytochromes b5 from insects and vertebrates. Proteins 67: 293–304

Xu J, Durr UH, Im SC, Gan Z et al (2008) Bicelle-enabled structural studies on a membrane-associated cytochrome B5 by solid-state MAS NMR spectroscopy. Angew Chem Int Ed Engl 47: 7864–7867